European Journal of Pharmaceutical Sciences 112 (2018) 195–206

Contents lists available at ScienceDirect

European Journal of Pharmaceutical Sciences

journal homepage: www.elsevier.com/locate/ejps

Poly(methyl vinyl ether-*co*-maleic acid) for enhancement of solubility, oral bioavailability and anti-osteoporotic effects of raloxifene hydrochloride

Jaleh Varshosaz[a,*], Mohsen Minaiyan[b], Ladan Dayyani[a]

[a] Department of Pharmaceutics, Faculty of Pharmacy and Novel Drug Delivery Systems Research Centre, Isfahan University of Medical Sciences, Isfahan, Iran
[b] Department of Pharmacology, Faculty of Pharmacy, Isfahan University of Medical Sciences, Isfahan, Iran

ARTICLE INFO

Keywords:
Electrospray
Raloxifene
Solubility enhancement
Poly(methyl vinyl ether maleic acid)
Oral delivery
Ovariectomized rats

ABSTRACT

Raloxifene HCl (RH) has poor water solubility and due to its extensive first pass metabolism; its bioavailability is only 2%. The purpose of the present study was to enhance the aqueous solubility, oral bioavailability and anti-osteoporotic effects of RH by electro-sprayed nanoparticles (NPs) in ovariectomized rats. NPs containing RH and different ratio of poly(methyl vinyl ether-*co*-maleic acid) (PMVEMA) were electrosprayed. The voltage, distance of needle to the collector, flow rate of the solution and polymeric percentage were optimized according to the size of NPs and drug solubility. The optimized formulation was characterized by SEM, XRD, DSC, and FTIR. The pharmacokinetic parameters were studies by oral administration of a single dose of 15 mg/kg in Wistar rats. The anti-osteoporotic effects were studied in female ovariectomized rats. Animals were treated with 6 mg/kg/day for 2 months then serum calcium, phosphorous and alkaline phosphatase levels were measured. RH loaded electrosprayed NPs showed 10-fold enhanced solubility compared to the free drug. Moreover, the XRD and SEM tests displayed an amorphous state of drug in the NPs. FTIR and DSC tests revealed no interaction between the polymer and the drug. Serum calcium, phosphorous and alkaline phosphatase levels were significantly decreased in ovariectomized rats receiving oral RH NPs ($P < 0.05$). No significant difference was detected between RH NPs and estradiol groups ($P > 0.05$). Oral bioavailability of NPs showed 7.5-fold increase compared to the pure drug. The electrosprayed PMVEMA nanoparticles can enhance solubility, bioavailability and antiosteoporotic effects of RH.

1. Introduction

Osteoporosis is a chronic world-wide disease and characterized by poor bone strength, low bone mass and micro-architectural deterioration of bone tissues (Roush, 2011). This is an age-related disease which occurs because of insufficient post-menopausal estrogen levels and misbalance between osteoblasts and osteoclasts (Sultan and Rao, 2011). Anti-resorptives are the major pharmacologic agents for osteoporosis which inhibit the development and action of osteoclasts (Jagadish et al., 2010). Numerous strategies such as hormone therapy, estrogen therapy, or a combination of estrogen and progesterone were frequently used in the past decades (Elsheikh et al., 2012). To date two major pharmacological approaches are reported for osteoporosis including anabolic agents such as parathyroid hormone which act via stimulating the bone formation process and administration of the anti-resorptive agents such as estrogen replacement therapy, calcitonin and RH which inhibits osteoclastic bone resorption (Silva and Bilezikian, 2011).

RH is the generic name for [6-hydroxy-2-(4-hydroxyphenyl) benzo-[*b*]thien-3-yl][4-[2-(1-piperidinyl)ethoxy]-phenyl]ethanone hydrochloride with a molecular weight of 510.05 g/mol (Bikiaris et al., 2009). It is a selective estrogen receptor modulator which is used for prevention and treatment of the osteoporosis (Tran et al., 2013). RH is also prescribed for breast cancer, prostate cancer, benign prostate hypertrophy and fibrocystic disease (Wempe et al., 2008). It belongs to class II of BCS (Biopharmaceutics Classification System) with poor water solubility due to its extensive first pass metabolism; the bioavailability of RH is only 2% (Shah et al., 2015). The solubility or dissolution of the drug in this category is therefore the rate-limiting step that determines the rate and extent of its absorption (Thakkar et al., 2011).

Approved dose of RH for oral administration for postmenopausal osteoporosis is 60 mg per day (Kushwaha et al., 2013). It is well documented there are cellular and molecular communications between estrogen and osteoblasts and osteoclasts activity (Uebelhart et al., 2009). Calciotropic and sex hormones are major regulators of bone growth, calcium and phosphate homeostasis (Uebelhart et al., 2009).

* Corresponding author at: Department of Pharmaceutics, Faculty of Pharmacy and Novel Drug Delivery Systems Research Centre, Isfahan University of Medical Sciences, Isfahan, PO Box 81745-359, Iran.
E-mail addresses: varshosaz@pharm.mui.ac.ir (J. Varshosaz), minayian@pharm.mui.ac.ir (M. Minaiyan).

https://doi.org/10.1016/j.ejps.2017.11.026
Received 10 October 2017; Received in revised form 25 November 2017; Accepted 28 November 2017
Available online 05 December 2017
0928-0987/

Solubility of a drug is an important factor to increase its oral bioavailability (Patil et al., 2013). Enhancement of oral bioavailability of poorly water soluble drugs is the most challenging aspect of drug development (Patil et al., 2013). Scientists have enhanced the aqueous solubility and dissolution of the poorly water-soluble pharmaceutical agents by different nanotechnology techniques (Yousaf et al., 2016). Pharmaceutical NPs may be produced by polymeric compounds (Jia et al., 2011). Natural polymers are more preferable for NPs formation because of the effectiveness, biocompatibility and biodegradation characteristics (Reis et al., 2006). There are several methods to develop pharmaceutical NPs including solvent evaporation, emulsification, phase inversion, solvent displacement and spray drying (Yousaf et al., 2016). However, disadvantages such as low yield, chemical decomposition of the drug, stability problems and environmental problems are reported for solvents (Newa et al., 2008). One of the newly introduced methods in production of pharmaceutical NPs is electrospraying technique (Luo et al., 2011). In this method at first the drug and polymer are dissolved in a solvent and the obtained transparent solution is subjected to electrospraying (Luo et al., 2011) which provides spherical NPs containing evenly scattered drug molecules in the polymeric matrix (Jia et al., 2011). Poly(methyl vinyl ether-*co*-maleic acid) (PMVEMA) is a hydrophilic and biocompatible polymer with mucoadhesive advantageous properties (Shahbazi et al., 2014). Kerdsakundee et al. (2017) used this polymer to improve the oral bioavailability of curcumin as a low water soluble drug. They modified halloysite nanotubes (HNT) with PMVEMA to endow it with mucoadhesive function for promoting drug absorption, and solubility. Afterward, the curcumin-loaded HNT was encapsulated in hydroxypropyl methylcellulose acetate succinate, as a pH-responsive polymer. Their results showed that PMVEMA significantly enhanced the interactions of HNT with the intestinal Caco-2/HT29-MTX cells and the mouse small intestines, and increased the permeability of curcumin across the co-cultured Caco-2/HT29-MTX cell monolayers by about 13 times compared to the free curcumin (Kerdsakundee et al., 2017).

It is hypothesized that RH can be used as an effective drug against osteoporosis if its bioavailability is enhanced (Yousaf et al., 2016). Even though numerous researches was been done to enhance the solubility and bioavailability of RH, still it is required to design the new formulations to improve release and avoiding first pass metabolism of this drug. So, the purpose of the present study was to develop novel electrosprayed NPs of RH with enhanced aqueous solubility, bioavailability and anti-osteoporotic effects for oral delivery in ovariectomized rats. To our knowledge there is no report on the use of PMVEMA in enhancement of solubility of drugs with emphasis on RH.

2. Materials and methods

2.1. Materials

The Raloxifene hydrochloride powder was kindly gifted by Iran Hormone Research Laboratories (Tehran, Iran). Poly(methyl vinyl ether-*alt*-maleic anhydride) (PMVEMA) [Mw: 216,000, pH 2.5 in H_2O] was from Sigma Company (US). *N*,*N*-dimethyl formamide (DMF) and all other reagents and chemicals were of analytical grade and obtained from Merck Chemical Company (Germany).

2.2. Preparation of nanoparticles by electro-spraying technique

Four different variables of the electrospraying technique including; voltage (12–20 kV), the distance between the tip of the needle to the collector (12–20 cm), flow rate of the solution (0.3–1 ml/h) and the polymer concentration (12–17 g/100 ml) were studied according to the preliminary tests and a hybrid surface response design using Design Expert Software (Version 7.1, US) was applied to optimize the parameters of the electrospraying technique. Initially total amount of the polymer and drug were dissolved in DMF according to Table 1. For instance in formulation M1 seen in Table 1, for 1 ml of the solution 188.3 mg of the polymer and 6 mg of drug were dissolved in 1 ml of DMF.

Table 1
Different formulations of RH nanoparticles prepared by electrospraying technique in a hybrid design.

Formulation code	A: Voltage (kV)	B: Distance (cm)	C: Rate (ml/h)	D: Polymer concentration (g/100 ml)
M1	16.00	16.00	0.65	18.83
M2	16.00	16.00	0.65	13.83
M3	12.00	12.00	0.30	16.01
M4	20.00	12.00	0.30	16.01
M5	12.00	20.00	0.30	16.01
M6	20.00	20.00	0.30	16.01
M7	12.00	12.00	1.00	16.01
M8	20.00	12.00	1.00	16.01
M9	12.00	20.00	1.00	16.01
M10	20.00	20.00	1.00	16.01
M11	22.07	16.00	0.65	11.88
M12	9.93	16.00	0.65	11.88
M13	16.00	22.07	0.65	11.88
M14	16.00	9.93	0.65	11.88
M15	16.00	16.00	1.18	11.88
M16	16.00	16.00	0.12	11.88

The collector of the electrospraying device included a standard aluminum foil (17 × 21 cm^2) which was placed as a cathode. 1 ml of the clear solution of the polymer and the drug was filled in a syringe fitted by a stainless steel nozzle with 23 gauge which acted as an anode. The condition of electrospraying was set up as shown in Table 1 and two responses including; particle size and saturation solubility of the studied formulations were measured. The solutions were extruded by the nozzle using a syringe pump (WPI, USA). After electrospraying, the nanoparticles on the collectors were carefully gathered and then the dry powder products were transferred into microtubes for further studies. A typical schematic of the electrospraying setup which was used to produce nanoparticles is shown in Fig. 1.

2.3. Particle size analysis

One milligram of nanoparticles of each formulation was dispersed in 6 ml of ethyl acetate and the particle size and particle size distribution of the nanoparticles was measured by photon correlation spectroscopy (PCS) (Zetasizer, ZEN 3600, Malvern Instrument, UK). The nanoparticles size was gained via a He-Ne laser beam at 658 nm at a fixed

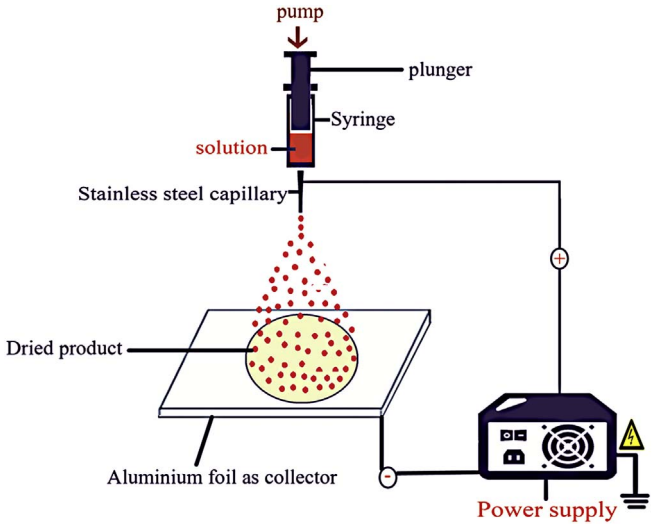

Fig. 1. Schematic representation of the electrospraying setup.

angle of 90° and the sample volume was maintained constant.

2.4. Saturated solubility

Saturated solubility of the pure drug and nanoparticles were obtained by Higuchi and Connoras (1965)'s method. For this purpose the ample amount of nanoparticles were dispersed in 5 ml of distilled water in a volumetric flask and the samples were agitated in a water bath for 1 min to obtain a homogeneous dispersion then stirred on a magnetic stirrer with the speed of 400 rpm for 24 h. After 24 h the samples were centrifuged (Eppendorf, Germany) at 10,000 rpm for 10 min. Subsequently, supernatants were filtered by a 0.22 μm filter membrane and the saturated solubility of each formulation was determined spectrophotometrically (UV-mini 1240, Shimadzu, Kyoto, Japan) at λ_{max} = 286 nm using the calibration curve of the free drug in aqueous medium. The results were compared to the saturation solubility of the pure drug.

2.5. Percentage yield

The discrepancy between the theoretical yield and the actual yield was calculated using the following equation:

$$\text{percentage yield}\,(\%) = \frac{\text{actual yield}}{\text{theoretical yield}} \times 100 \quad (1)$$

2.6. Fourier transform infrared spectroscopy (FTIR)

To determine the potential physical or chemical interaction between the polymer and the drug, the FTIR spectra of pure drug, polymer and nanoparticles of RH were recorded on the FTIR spectroscope (Jasco, FTIR model 6100, Japan) by using a potassium bromide pressed disc method and scanned in the wave numbers ranging from 400 to 4000 cm^{-1}.

2.7. Scanning electron microscopy (SEM)

To mount the samples on an aluminum stub, a double-sided adhesive tape was used. Then the coat procedure was done under vacuum with gold in an argon atmosphere. The morphology of the samples was studied by an SEM (Hitachi F41100, Japan).

2.8. X-ray powder diffraction (XRPD)

The XRPD test was executed for the crystallinity of the samples. The ground sample powder was filled into the sample holder of the X-ray diffractometer (Philips, Netherland) and then smoothed with a spatula. X-ray diffraction patterns of pure drug, polymer and nanoparticles of RH were obtained at 40 kV and 30 mA over a range of (2q) between 10°–60° by exposing the samples to Cu Kα radiation.

2.9. Thermal analysis (DSC)

Differential scanning calorimetric (DSC) test was done to define potential mismatches among the drug, the polymer and nanoparticles. 3–6 mg of the samples were used for recording the thermograms by a DSC device (822e Mettler-Toledo, Switzerland) equipped with a refrigerated cooling system. The DSC was calibrated with indium standard. The scan was conducted between 20 and 300 °C at a heating rate of 10 °C/min using an aluminum pan enclosed with a lid under a nitrogen purge. A similar empty pan was used as the reference. The software (STARe Ver. 10.00 Mettler Toledo, Switzerland) of the device was used to record the melting point of the sample.

2.10. Drug content determination of the optimum formulation

In order to calculate the entrapment efficiency of RH within the RH nanoparticles 10 mg of the optimum formulation was dissolved in 5 ml of methanol. The resulting solution was centrifuged at 10,000 rpm for 10 min. Afterwards, the supernatant was passed through 0.22 μm filter membrane and the absorption of the filtrate was quantified after suitable dilution at 287 nm spectrophotometrically. The real concentration of RH in the formulation was measured by the standard curve of RH in methanol. A solution of blank, containing just the polymer, was used to have the assurance that the absorption was just related to the drug. Entrapment efficiency (EE) was determined by means of the proportion of the drug existing in the nanoparticles and was considered as the trapped drug. The EE and loading efficiency (LE) of RH-loaded nanoparticles were determined using the following equation (Anitha et al., 2011):

$$EE\,(\%) = \frac{entrapped\ drug}{total\ drug} \times 100 \quad (2)$$

$$LE\,(\%) = \frac{entrapped\ drug}{amount\ of\ polymer + drug} \times 100 \quad (3)$$

All the measurements were performed in triplicate.

2.11. Dissolution rate studies

In vitro dissolution studies were performed by comparing the release of pure drug with the optimized formulation. Therefore, to keep the sink condition, 30 mg of nanoparticles equivalent to 1.3 mg of the drug which was < 15% of the saturated solubility of RH in nanoparticles was dispersed in 1 ml of deionized water and was appropriately enclosed at both ends in a dialysis bag (cutoff 12,000 Da). This procedure was repeated for pure drug (1.3 mg) and the polymer as the blank sample (28.7 mg). Loaded bags were dipped into 49 ml of deionized water which was constantly rotated at 400 rpm on the magnetic stirrer (IKA-WERKE, Model RT 10 power, Japan). The whole compartment was sealed off to avoid vaporization of the dissolution medium. At certain time intervals, 1 ml of dissolution medium was withdrawn and analyzed using the UV spectroscopy at 286 nm. For each sample, the dissolution test was done in triplicate. Moreover, the dissolution efficiency up to 30 min (DE) was enumerated according to the following equation:

$$DE_T = \frac{\int_0^T y_t \cdot dt}{y_{100} \cdot T} \quad (4)$$

2.12. Animal studies

2.12.1. Anti-osteoporotic effects of RH nanoparticles in ovariectomized rats

Thirty six adult female Wistar rats (200–250 g) were randomly divided into 6 experimental groups (n = 6). Animals were housed under standard laboratory conditions in agreement with European community regulations for laboratory animals (ambient temperature 22 ± 1 °C, 12 h dark/light cycle). All protocols were approved by the institutional animal ethical committee guidelines of the Health Ministry of Iran (the reference of approval number of animal ethical committee was 394,690), and chow pellets and water were provided ad libitum. The animals were housed individually at a room temperature of 25 ± 2 °C with relative humidity of 50–60% and on 12 h light/12 h dark cycles in the animal house. Before ovariectomy, the animals were anesthetized using intra-peritoneal ketamine HCl and xylazine injection at doses of 50 mg/kg and 10 mg/kg body weight, respectively. Their abdomens were shaved, and the skin was cleaned using 70% ethanol followed by povidone-iodine (Betadine) solution. Bilateral dorsal incisions were made on the back. The ovaries were found. The ovarian arteries were

Table 2
Physical properties of RH nanoparticles obtained from electrospray technique. Values are expressed as mean ± SD; n = 3.

Formulation code	Particle size (nm) ± SD	PDI ± SD	Percentage yield (%) ± SD	Water solubility (μg/ml) ± SD
M1	326.9 ± 65.9	0.44 ± 0.09	86.7 ± 9.1	146.7 ± 41.3
M2	172.3 ± 66.7	0.40 ± 0.06	78.6 ± 9.0	192.5 ± 21.0
M3	248.0 ± 147.7	0.81 ± 0.06	80.3 ± 4.2	161.4 ± 1.5
M4	374.3 ± 45.1	0.50 ± 0.03	75.6 ± 3.4	209.1 ± 40.7
M5	434.2 ± 104.9	0.68 ± 0.04	62.7 ± 6.1	123.2 ± 18.1
M6	396.1 ± 55.8	0.36 ± 0.06	74.4 ± 1.7	132.1 ± 24.7
M7	539.0 ± 171.4	0.85 ± 0.10	86.4 ± 12.4	215.5 ± 31.0
M8	305.9 ± 26.1	0.29 ± 0.07	56.4 ± 9.4	102.3 ± 48.2
M9	317.4 ± 42.5	0.43 ± 0.20	80.2 ± 7.8	230.0 ± 3.5
M10	429.6 ± 95.1	0.69 ± 0.08	77.9 ± 7.4	216.0 ± 7.5
M11	479.3 ± 32.4	0.24 ± 0.01	57.2 ± 7.6	140.9 ± 45.2
M12	1746.2 ± 1572.2	0.98 ± 0.02	17.5 ± 1.8	122.5 ± 9.7
M13	224.2 ± 26.8	0.29 ± 0.03	54.3 ± 6.0	203.9 ± 13.5
M14	285.8 ± 48.0	0.41 ± 0.05	73.8 ± 2.0	222.6 ± 13.2
M15	209.9 ± 47.5	0.43 ± 0.02	66.0 ± 12.2	215.9 ± 22.4
M16	570.1 ± 91.9	0.61 ± 0.07	82.1 ± 15.7	160.6 ± 17.9

ligated. The connection between the fallopian tube and the uterine horn was cut and the ovaries were moved out. The muscle layer was sutured and the skin incision was closed with silk suture. To ensure almost complete clearance of their bodies from estrogen hormone residues, 4 weeks lasted to complete surgical recovery operation.

Anti-osteoporotic effect of RH nanoparticles was studied after oral administration of 6 mg/kg of the drug for 8 weeks in 6 groups of animals. The studied groups included; group 1: un-ovariectomized and untreated (sham group), group 2: ovariectomized without treatment, group 3: ovariectomized and treated by oral administration of pure polymer (33.5 mg/day), group 4: ovariectomized and orally administrated with pure drug (6 mg/kg/day), group 5: ovariectomized and orally administrated with estradiol valerate (1 mg/kg/day) and group 6: ovariectomized and orally administrated with RH nanoparticles (35 mg/day equal to 6 mg/kg/day of the pure drug). Twenty six days after ovarectomy serum calcium (Ca), phosphorous (P) and alkaline phosphatase (ALP) levels were determined in all animals. Then treated for 60 days and serum Ca, P and ALP levels were measured using commercial detecting kits (Pars Azmoon Co. and BioRexFars Co.) by auto analyzer (Mindray-BS-200, Germany).

2.12.2. Pharmacokinetic studies

The rats were kept fasted 12 h before and 4 h after drug administration and just had free access to the water. Then they were divided into 2 groups and were orally administered a single dose of 15 mg/kg of the pure drug or RH nanoparticles (Shah et al., 2016). Then the rats were anesthetized with ether and blood sampling was done by inserting a heparinized capillary into the retro-orbital vein to get 0.5 ml of blood at a time interval of 0.083, 0.25, 0.5, 1.0, 2, 4, 8, 12, and 24 h. The samples were centrifuged at 5000 rpm for 15 min and the plasma was separated and frozen immediately at − 20 °C until analysis by the HPLC method.

2.12.3. Plasma sample preparation

To 100 μl of plasma sample 100 μl of methanol and 300 μl of acetonitrile were added and vortex-mixed for 20 s and the sample was centrifuged at 15000 rpm for 10 min to separate the denatured proteins. Twenty microliter of the supernatant was injected into the HPLC for analysis. The pharmacokinetic parameters including C_{max}, T_{max}, AUC_{0-24}, $AUC_{0-\infty}$, K_a, K_{el} were calculated and compared to the pure drug and the nanoparticles.

2.12.4. HPLC analysis method

A reversed-phase HPLC method was used to measure the plasma concentration of the drug. HPLC (Waters, 5.5, USA) device with two pump and UV detector were used. Mobile phase consisted of acetonitrile, ammonium acetate (pH 4.0, 0.05 M) (50:50% v/v) with a flow rate of 0.8 ml/min to elute the drug. The mobile phase was filtered through 0.45 μm nylon filters (Millipore, USA) and the samples were analyzed at λ_{max} 289 nm.

2.13. Statistical analysis

The Design Expert Software (version 7.1, Stat-Ease, Inc., Minneapolis, MN, US) was used for designing and optimization of the nanoparticle formulations. Using this software the main effects and interaction effects of the factors on each response was individually determined. Obtained data were analyzed using analysis of variance (ANOVA) followed by a post hoc test of LSD and presented as mean ± SD.

3. Results

3.1. Physical properties of nanoparticles

The results of particle size, saturation solubility and yield percent of different studied formulations are shown in Table 2.

3.1.1. Particle size measurement

The particle size of the RH nanoparticles of different formulations is shown in Table 2. According to the data, in all formulations the particle size was < 1000 nm but only in formulation of 12 the particle size was > 1000 nm.

Fig. 2 shows the effect of the combination of the studied variables of the electrospraying method on the particle size of the nanoparticles.

Based on analysis using Design Expert Software and using the hybrid model, the following equation was achieved for particle size:

$$\begin{aligned}\text{Particle size} = {} & 191.132 - 3.38A - 1.22B + 17.59C - 6.13D + 7.55AB \\ & - 22.98AC - 9.02AD + 30.40BC + 4.71BD - 0.59CD \\ & - 23.24A2 + 12.16B2 + 1.30C2 - 11.35D2 \end{aligned} \quad (5)$$

where, A, B, C and D are the voltage, distance of the tip of the needle to the collector, rate and polymeric concentration respectively.

Positive signs in this equation reflect a boost of the response by the experimental variable, while a negative sign means the experimental variable castrate the impact. Statistical analysis showed that lower values of voltage caused larger particle size but insignificantly ($P > 0.05$) except for the voltages lower than 10 kV which had significant effect on the particle size ($P < 0.05$). Increasing or reducing the values in other variables had no distinct differences on particle size ($P > 0.05$).

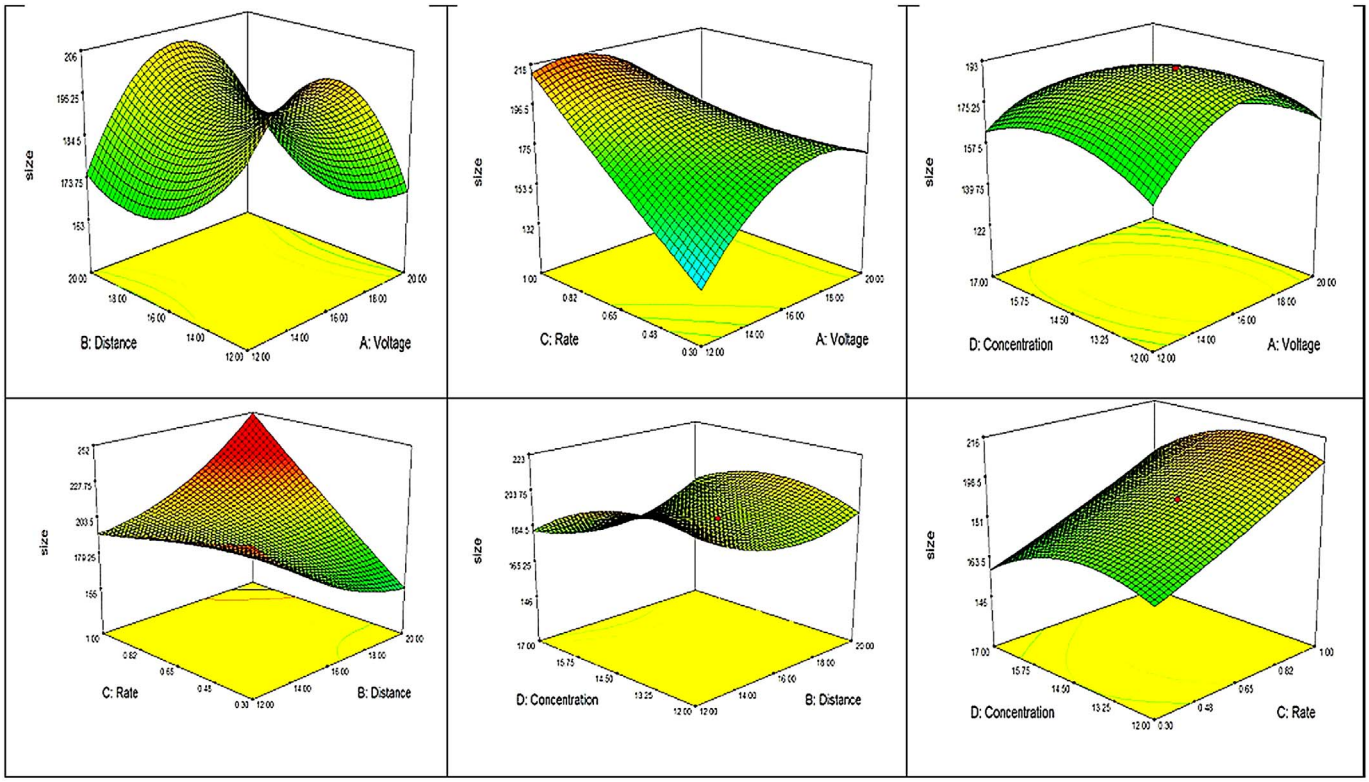

Fig. 2. 3-D plots showing relative effects of the combination of studied variables of electrospraying method on particle size of raloxifene HCl nanoparticles.

3.1.2. Saturation solubility studies

The saturation solubility of the pure RH was 19.88 ± 0.12 μg/ml which is categorized as a poor water soluble compound. As Table 2 shows the saturation solubility of all studied formulations was significantly increased in comparison with the pure drug ($P < 0.05$). Fig. 3 shows the effect of the combination of the studied variables of the electrospraying method on the saturation solubility of RH.

Final equation in terms of coded factors was suggested by Design Expert software to predict the solubility of the nanoparticles:

$$\text{Solubility} = 134.87 - 155.12A + 1.33B - 32.31C - 105.52D + 22.62AB - 26.13AC + 249.83AD - 38.23BC + 20.59BD + 82.25CD + 316.64A2 - 55.72B2 + 2.88C2 + 124.97D2 \quad (6)$$

In which A, B, C and D are as defined already.

According to the statistical analysis of the data of Table 2, this response increased significantly with a reduction of the polymer concentration and increasing the other variables ($P < 0.05$). Furthermore, it could be concluded that the polymer concentration and voltage had

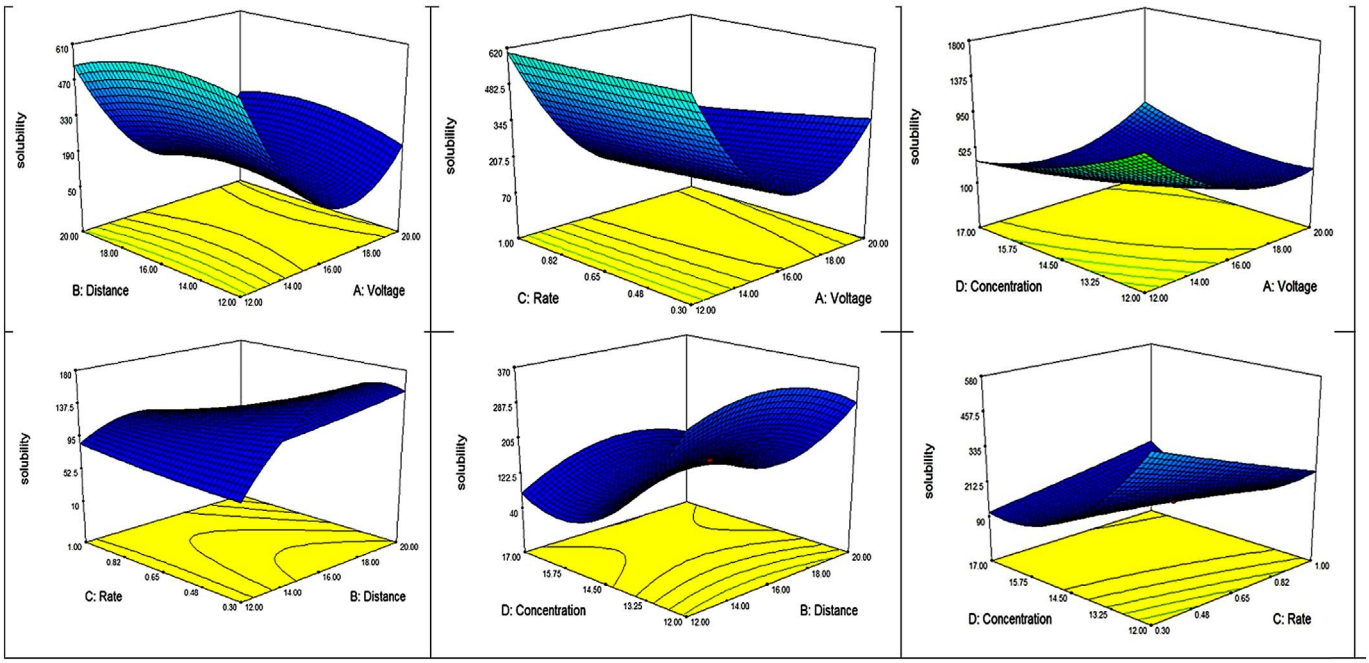

Fig. 3. 3-D plots showing relative effects of the combination of studied variables of electrospraying method on saturation solubility of raloxifenHCl nanoparticles.

more influence on solubility than the other two parameters. However, the distance of the tip of the needle to the collector had less effect on solubility.

3.1.3. Percentage yield outcomes

The results of the percentage yield outcomes are presented in Table 2. Based on the results, the formulation 7 had the higher yield than others while the formulation 12 had the least yield percentage compared to the other formulations. There was no specific relation between the studied variables and the percentage yield. However, it was observed that the voltages lower than 10 kV caused very low yield.

3.2. Optimization of the formulation of RH nanoparticles

The voltage, distance of needle to the collector and flow rate of the solution and polymeric percentage were optimized according to the size of the nanoparticles and drug solubility. Design Expert Software was used to determine the effect of the levels of independent variables on the studied responses. The optimum condition for electrospraying was achieved at the voltage of 18.24 kV, the concentration of polymer at 13%, the distance of needle to the collector of 19.69 cm and the flow rate of 0.43 ml/h. In this situation, the particle size and saturated solubility for the optimum formulation were 201.7 ± 62.6 nm and 219.9 ± 14.7 μg/ml, respectively. The PDI of the optimum formulation was 0.26 and its saturation solubility was 219.9 ± 14.7 μg/ml which shows about 10-fold enhancement compared to the pure drug. Table 3 shows the actual values of the characteristics of the optimized RH nanoparticles in comparison with the predicted values by the software.

3.3. Fourier transforms infrared spectroscopy

As seen in Fig. 4a, the main peaks for drug were seen at 3141.47, 2954.41, 1641.13, 1596.81 cm^{-1} for phenolic OH, aliphatic C—H, C═O and C—O—C bounds, respectively. Also, for S of benzothiofuran, C—N, C—O and aromatic = CH the peaks were seen at 1464.67, 1360.53, 1264.11 and 836.955 cm^{-1}, respectively. The main peak for RH nanoparticle on OH, aliphatic C—H, S of benzothiofuran, C═O, C═C, C—N and C—O ether bounds were detected at 3450.03, 2940.91, 1436.71, 1722.12, 1648.05, 1386.57 and 1180.22 cm^{-1}, respectively (Fig. 4b). The main peaks for polymer was seen on the OH, C═O and C—O ether bounds at 3493.38, 1712.48 and 1177.33 cm^{-1}, respectively (Fig. 4c). The presence of all functional peaks of the drug in the nanoparticles' spectra showed that there was no significant physicochemical interaction between the drug and the polymer in the optimized formulation.

3.4. Morphology of nanoparticles (SEM)

As observed in Fig. 5 the particles of the RH are presented in cubic shape. Also, the nanoparticles size was < 300 nm with spherical form which is almost in accordance to the results of DLS method.

3.5. X-ray powder diffraction

The XRD results for the nanoparticles, polymer and drug are presented in Fig. 6. As seen in Fig. 6a there was no obvious peak for the pure polymer as well as the RH nanoparticles (Fig. 6b) while the pure drug showed typical peaks at 21.4°, 22.6°, 39.9° which indicates drug encapsulation in nanoparticles has changed the crystalline habit of the drug from the crystalline to amorphous form.

3.6. Thermal analysis (DSC) studies

Based on the Fig. 7, the DSC of the RH nanoparticles, pure polymer and pure drug are presented in Fig. 7. In thermogram of the pure drug a

Table 3
The comparison of the predicted and actual values of different characteristics of the optimum formulation of the RH nanoparticles. Values are expressed as mean ± SD; n = 3.

Formulation code	Particle size (nm) ± SD	PDI ± SD	Percentage yield (%) ± SD	Water solubility (μg/ml) ± SD	Entrapment efficiency (%) ± SD	Drug loading (%) ± SD
Actual	203.3 ± 10.6	0.26 ± 0.04	86.2 ± 9.0	219.9 ± 14.7	97.1 ± 17.1	4.5 ± 0.8
Predicted	174.1	–	–	220.2	–	–
Error%	16.7	–	–	−0.13	–	–

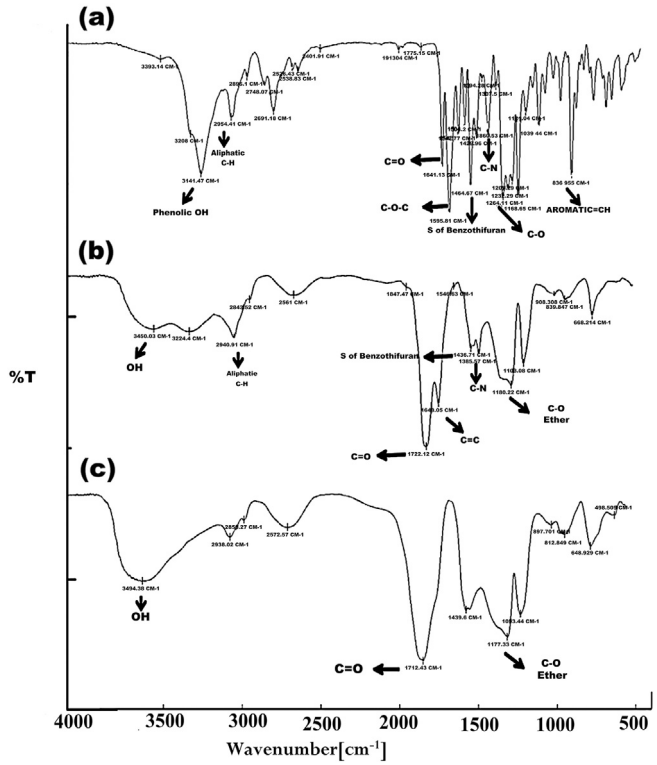

Fig. 4. The FTIR spectroscopy results of a) pure raloxifene HCl, b) RH nanoparticles, and c) pure PMVEMA.

peak at 263.7 °C was seen which related to the melting point of the drug (Fig. 7a). For the polymer, 2 peaks were detected at 149.9 and 159.5 °C which are related possibly to the glass transition temperatures (Tg) of a mixture of acidic and anhydride forms of the polymer presented at the sample (Fig. 7b). Also, for the nanoparticles two peaks were observed at 82.1 and 142.9 °C (Fig. 7c). The peak seen at 82 °C was related to the polymer and can be seen in the pure polymer thermogram too (Fig. 7b) and the peak at 142.9 °C related also to the Tg of the polymer. However, no distinct peak showing the melting point of the drug was detectable in the nanoparticles thermogram which shows probably the amorphous state of the drug in the nanoparticles (Fig. 7b).

3.7. Dissolution studies

The dissolution profiles of the pure drug and RH nanoparticles are presented in Fig. 8. A significant difference was detected on drug release percentage at 30 min between the pure drug and the nanoparticles, so that after 10 min approximately 95% of the RH was dissolved from its nanoparticles while only 11% of the pure drug was dissolved ($P < 0.05$).

3.8. Animal studies

3.8.1. Serum calcium level

The effect of oral delivery of the novel electrosprayed RH nanoparticles on serum calcium in ovariectomized rats is presented in Fig. 9a. The calcium levels were significantly increased in ovariectomized rats ($P < 0.05$) compared to the normal group. Also, serum calcium levels significantly decreased in ovariectomized rats which were treated with pure drug compared to the control group (ovariectomized-untreated) ($P < 0.05$). Moreover, serum calcium levels significantly decreased in ovariectomized rats treated with RH nanoparticles compared to the other groups ($P < 0.05$). No significant difference was detected between ovariectomized rats treated with RH nanoparticles and those treated by estradiol ($P > 0.05$).

3.8.2. Phosphorus level

According to the Fig. 9b, serum phosphorus levels significantly decreased in ovariectomized rats treated with RH nanoparticles compared to the other groups ($P < 0.05$). Also, no significant difference was detected between ovariectomized rats treated with RH nanoparticles and estradiol valerate group ($P > 0.05$).

3.8.3. Alkaline phosphatase (ALP) level

According to the results of Fig. 9c, serum ALP significantly decreased in ovariectomized rats treated with RH nanoparticles compared to the other groups ($P < 0.05$). Also, there was no significant difference between ovariectomized rats treated with RH nanoparticles and estradiol valerate group ($P > 0.05$). The effect of oral delivery of the novel electrosprayed RH nanoparticles on ALP level in ovariectomized rats is presented in Fig. 9c.

3.8.4. Pharmacokinetic studies

Fig. 10 shows the serum concentration-time profiles of untreated RH and the optimized nanoparticles. The figure shows a two-compartment model for the pharmacokinetic of RH in serum of rats. As it is indicated in Table 4 there are significant differences between C_{max}, T_{max}, AUC_{0-24}, $AUC_{0-\infty}$, K_{el} and K_a of nanoparticles of RH and untreated drug at similar doses ($P < 0.05$). The rats administered by nanoparticles showed the values of C_{max} and K_a as much as 11.7 ± 3.0 μg/ml and 8.34 ± 2.16 h^{-1}, respectively. Whereas these values were 0.485 ± 0.13 μg/ml and 0.29 ± 0.10 h^{-1} for untreated RH. Increased specific surface area of nanoparticles of drug due to its decreased particle size can explain the enhanced dissolution rate, solubility and decreased crystallinity of RH which in turn led to increased blood concentration and decrease the T_{max} of drug nanoparticles in comparison to the untreated drug. The nanoparticles showed a 7.5 fold greater AUC_{0-24} compared to the untreated drug which means that the relative bioavailability of RH has improved significantly ($P < 0.05$).

4. Discussion

Electrospraying is a multipurpose method to produce the nanoparticle based coatings for various applications using electrical charges (Zamani et al., 2016). Electrospraying provides spherical nanoparticles containing evenly scattered drug molecules in the polymeric matrix (Jia et al., 2011). Coating using this method provides a thin layer for biomedical devices. In this regard, to improve osteogenesis electrospray of orthopedic implants coated with osteogenic compounds was previously reported by Hu et al. (2013).

Electrospraying is a unique technique to produce a layer of coating on 3-D structures and to the best of our knowledge, scarce researches have done to fabricate electrospray-based drugs for osteoporosis. So, in this study we enhanced solubility, dissolution rate and oral bioavailability of a poorly water soluble drug like RH by oral delivery of its novel electrosprayed nanoparticles. All developed formulations of the RH loaded nanoparticles showed remarkably enhanced solubility compared to the free drug (Table 2). The solubility improved about 10-fold higher than that of the pure drug. The electrospray procedure and resulting droplet sizes are controlled by the process parameters that include the applied voltage, liquid flow rate, and liquid properties (Jaworek, 2007). It is expected that the electrospraying method produce spherical nanoparticles (Suthar et al., 2011) as the SEM images revealed spherical shapes for RH nanoparticles (Fig. 5b). It is worth mentioning that electrospraying happens at the semi-dilute entangled state of the polymer, which resulted in the formation of spherical and monodispersed particles (Zhou et al., 2016). Various structured particles have been produced via electrospraying technique, including poly (methyl-methacrylate)-pigment nanoparticles, microbubble suspensions, cholesterol nanoparticles, so on (Wu et al., 2012). In comparison with conventional technologies, it is assumed that electrospraying is an efficient method to produce nanoparticles for drug delivery (Wu et al.,

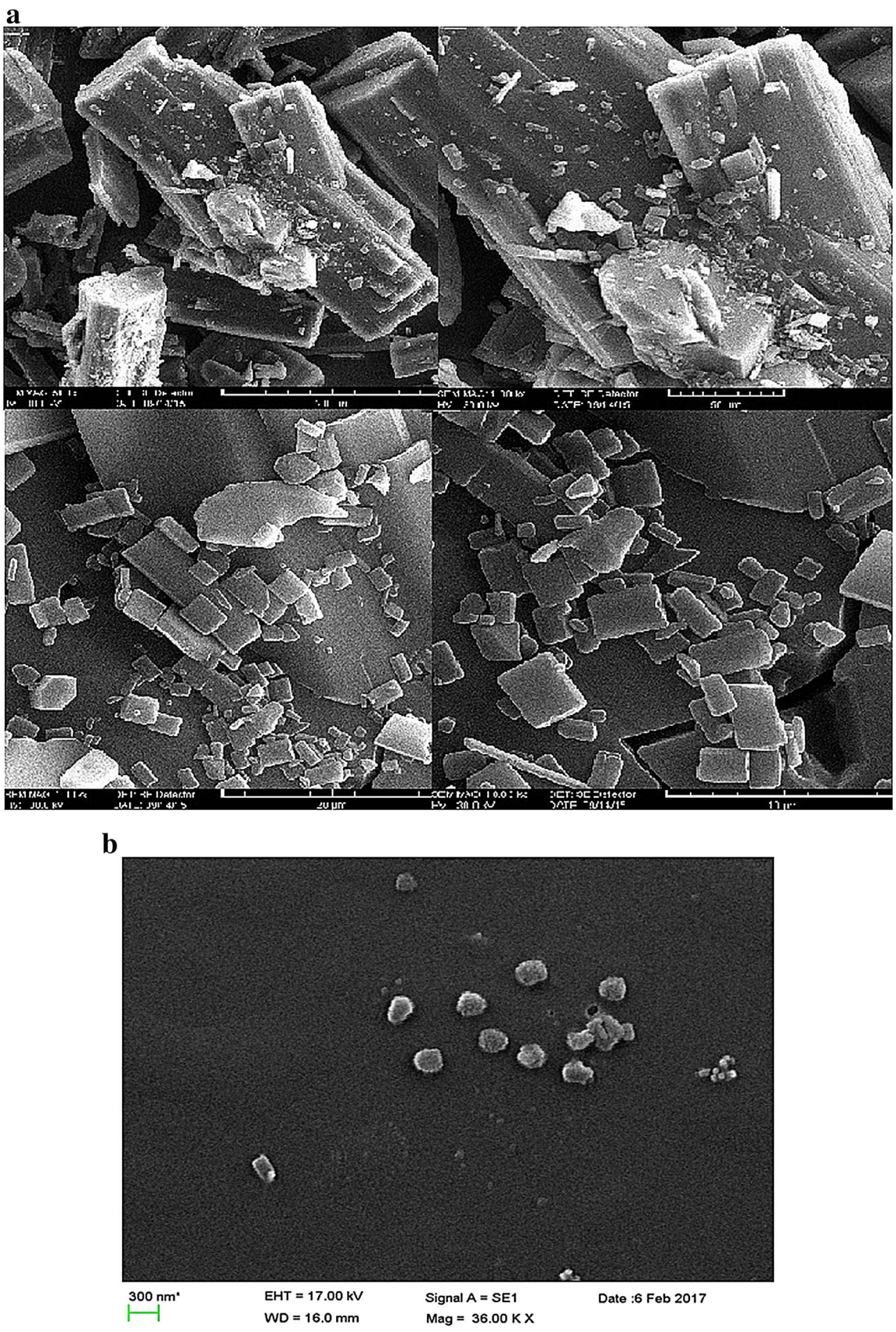

Fig. 5. The SEM micrographs of a) RH and b) RH nanoparticles with magnification of × 5000.

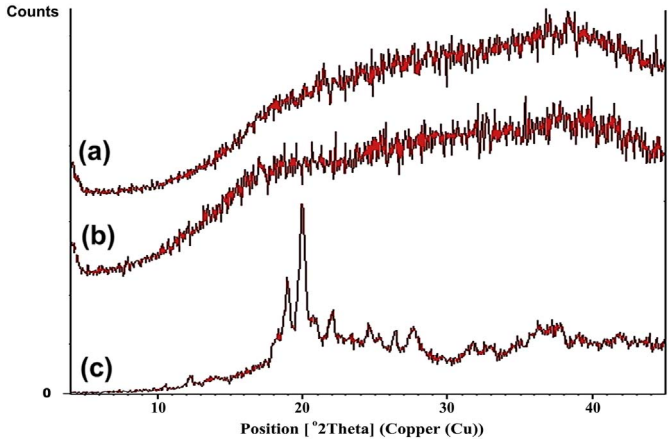

Fig. 6. The XRD diffractograms for the a) RH nanoparticles, b) pure PMVEMA and c) pure RH.

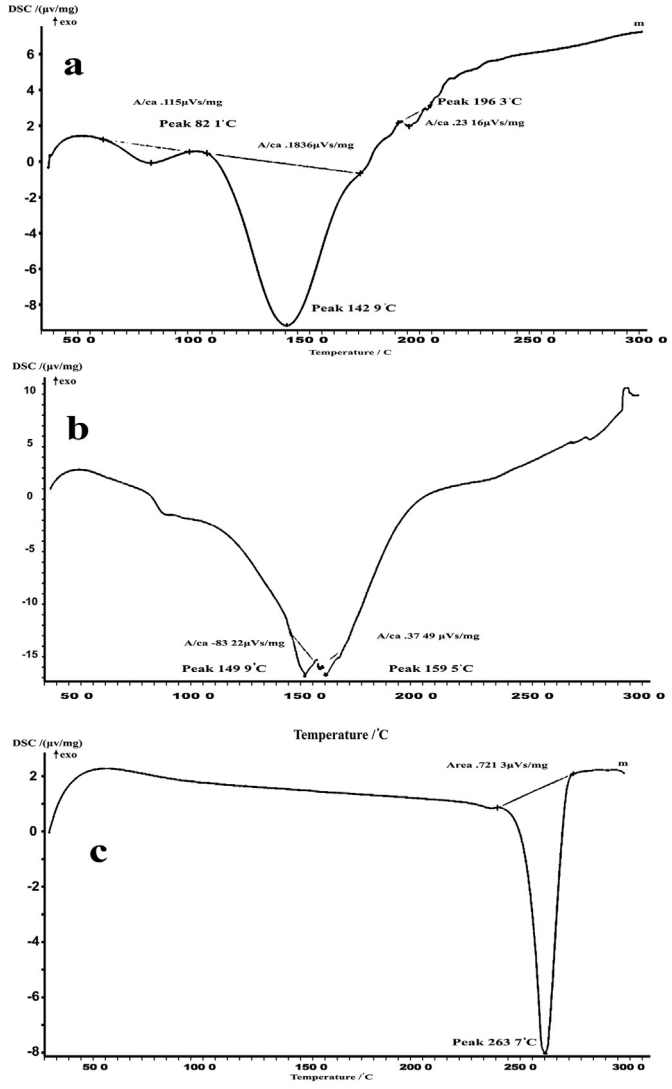

Fig. 7. The DSC thermograms of the a) RH nanoparticles, b) pure PMVEMA and c) pure RH.

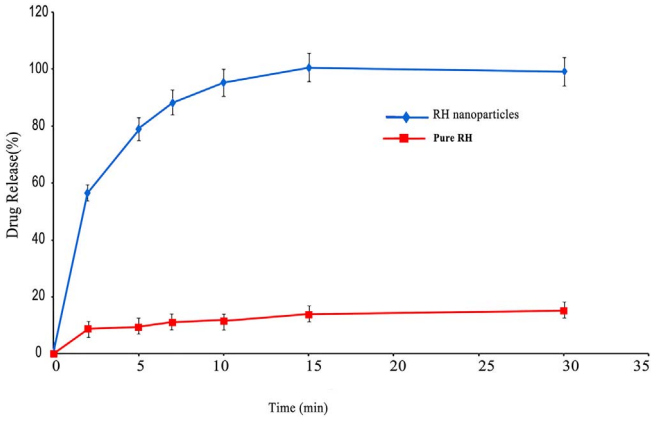

Fig. 8. The dissolution profile of the pure drug versus optimized RH nanoparticles prepared by electrospraying method (n = 3). The results are shown as mean ± SD.

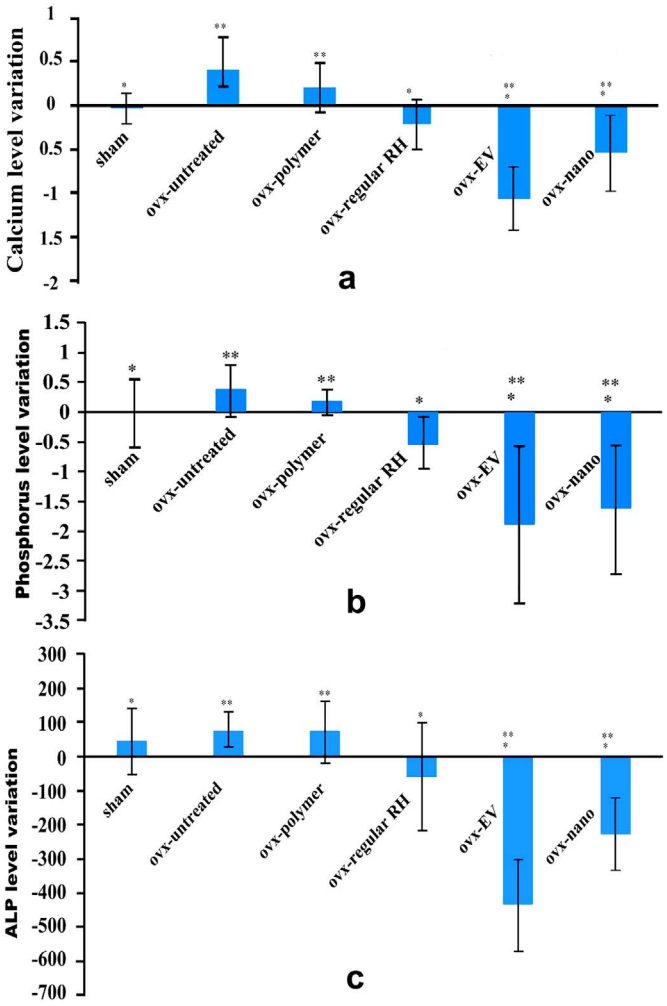

Fig. 9. The effect of oral delivery of the pure or electrosprayed RH nanoparticles on serum levels of a) calcium, b) phosphorous and c) alkaline phosphatase in ovariectomized rats (n = 6). The results are shown as mean ± SD. (*) shows the significant difference (P < 0.05) with the untreated ovariectomized rats and (**) shows the significant difference (P < 0.05) with the pure drug.

2012). This method is an electrohydrodynamic atomization technique which is simple, cost-effective, scalable, flexible, reproducible and effective method to produce particles at the nanoscale with narrow size distribution, spherical shape and tailored morphology. This is suggesting that electrospraying could be as one of the most reliable and well-practiced methods to be indicated in many pharmaceutical fields. For example, it can improve the bioavailability of poorly water soluble drugs and prepare targeted drug delivery systems (Nguyen et al., 2016; Sosnik, 2014). By electrospraying method, single-step monodisperse

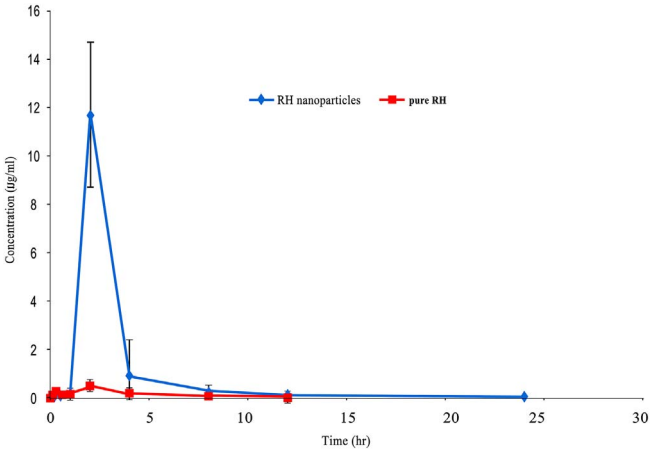

Fig. 10. Plasma concentration-time profiles of RH after oral administration of 15 mg/kg RH powder and equivalent amounts of optimum nanoparticles in rats (n = 6). The results are shown as mean ± SD.

nanoparticles are produced in powder form for drug delivery with high loading and reliable dissolution profiles. The procedure can be done at room temperature and without coagulation chemistry (Pathak et al., 2016; Alehosseini et al., 2017; Trotta et al., 2010). Electrosprayed nanoparticles can be used as a high density sinking dosage form which can enhance gastric retention because the nanoparticles can sink to the bottom of the stomach near the pylori sections (Hao et al., 2014). During the electrospraying method, use of an external dispersion/emulsion phase is not required for biomedical indications (Arya et al., 2009). Furthermore, it is proven that electrospraying is a promising method to prepare amorphous nanoparticles and a certain approach to improve the oral bioavailability of poorly water soluble drugs (Smeets et al., 2017). Electrospray has great potential to produce nanoparticles for a variety of drug/nucleic acid delivery applications, including solid lipid nanoparticles for hydrophobic drug delivery, as well as polyplexes and lipoplexes for nucleic acid delivery (Wu et al., 2012).

The characteristics of electrosprayed particles are still not completely understood and it is important to proceed in a step-wise manner intended to understand the relationship between processing parameters and characteristics of electrosprayed microparticles before one progresses to the inclusion of highly fragile and expensive bioactive molecules (Bock et al., 2011).

As inferred in our study based on Eq. (5) and Fig. 2 the main parameters which influenced the particle size of nanoparticles were flow rate and polymeric concentration although the effects were not significant ($P > 0.05$). This is in accordance with previous studies (Bock et al., 2011). It is expected that the viscosity of the polymer has a direct effect on the particle size (Moghadam et al., 2009) so that, by reducing the polymeric concentration, the viscosity decreased and consequently this leads to smaller particle size. Nevertheless this is in contrary to the Eq. (5) obtained by Design Expert software. In this equation the polymeric concentration shows an antagonist effect on size which means that, by increasing the concentration, the particle size has decreased. Hartman et al. (2000) reported that polymeric concentration affected the surface tension of the solution and caused micro-dripping style of electrospraying. They suggested that particle size increased with decreasing the surface tension. The surface tension increased due to two main reasons: increase in polymer content and decreasing the flow rate of solution. Moreover, the lower concentration of the polymer in the solution, the weaker the entanglement of the polymer molecules (Hao et al., 2006) and possibly this caused to larger droplet size. This could explain the results attained in our study shown in Eq. (5). In our study the range of the polymeric concentration and flow rate were narrow however, at broader range this conclusion may be obtained more significantly. Interestingly at the voltages below 10 kV (formulation M12) the particle size changed significantly (Table 2). Regardless of flow rate and polymeric concentration; at 10 kV, particle size was significantly larger than higher voltages (Table 2). Probably, high voltages could cause ejection of smaller fraction of offspring droplets and the final nanoparticles size got lower. Perhaps by applying the high voltages, the viscosity decreased due to the fact that the polymer solution is shear-thinning fluid and the viscosity has a direct relation with particle size. Furthermore, at high voltages, dripping mode dominated over the jet mode caused faster formation of droplets while the size of droplets reduced. At the higher voltages, stronger electric field obligated the Taylor-cone to collapse and break into smaller droplets (Bock et al., 2011; Moghadam et al., 2009; Zhou et al., 2016). However, the limitation must be applied since the onset of an unstable jet. This constraint allows stable jet led to better repeatability and reproducibility (Zhou et al., 2016).

Poor water-solubility of drugs is still a serious problem in pharmaceutical formulations, affecting its quality and drug bioavailability. So, one of the most challenging tasks in the pharmaceutical industries is to improve solubility of these drugs (Kakran et al., 2011). Following oral administration of drugs in class II, the limited wetting properties and therefore poor dissolution rate of these drugs into the fluids of gastrointestinal tract limits their in vivo performance (Kakran et al., 2011). As seen in Fig. 3 the voltage and polymeric concentration are the most important parameters which can affect the solubility. The solubility enhanced by diminishing the particle size (Narayan et al., 2017). As discussed before higher voltages and lower flow rates could result in smaller particle size. This is observed in Fig. 3 and confirmed the Eq. (6). But the paradox is about polymeric concentration. Increasing the polymer resulted in smaller particle size but decrease the solubility. Fig. 3 shows that initially increase in the polymer content from the range of 12–14 g/100 ml led to enhancement of the solubility but increasing excess than this range decreased the solubility. One of the probabilities is that by increasing the concentration, the spherical shape and surface morphology of the nanoparticles changed (Zhou et al., 2016) and this may affect the solubility. The polymeric concentration of the optimum formulation was 13%. Additionally the drug changes into amorphous form during the electrospraying method (Fig. 6). Thus it can be inferred that electrospraying could produce nanoparticles in which the RH transforms its crystalline habit. Other studies in which electrospraying method was employed on different drugs such as fenofibrate (Yousaf et al., 2016), triamcinolone acetonide (Jahangiri et al., 2014), CoQ10 (Fung et al., 2016) confirmed our results. As the matter of fact, the amorphous state of the drug can increase the solubility and dissolution rate (Patil et al., 2013). As observed in this study, the RH loading and release increased in comparison with the other reported methods like solvent emulsification/evaporation method reported by Kushwaha et al. (2013). In Kushwaha et al. (2013) study nearly 100%

Table 4
Pharmacokinetic parameters of pure RH in comparison with the optimum nanoparticles obtained from electrospraying method.

RH type	C_{max} (µg/ml)	T_{max} (min)	K_a (h^{-1})	K_{el} (h^{-1})	AUC_{0-24} (µg·h/ml)	$AUC_{0-\infty}$ (µg·h/ml)
Pure RH	0.485 ± 0.13	240.0 ± 0.0	0.29 ± 0.10	0.017 ± 0.006	3.19 ± 0.87	3.19 ± 0.87
RH nanoparticles	11.73 ± 3.00*	120.0 ± 0.0*	8.34 ± 2.16*	0.11 ± 0.004*	22.97 ± 9.43*	23.61 ± 8.88*

Note: Each value represents the mean ± SD (n = 6).
* $P < 0.05$ shows significant difference compared to the pure RH powder.

of the drug release occurred within 4 h but in our study after 10 min approximately 95% of the RH was dissolved. RH solubility enhanced nearly five times than the pure drug in their study while the solubility of RH increased about 10 fold in comparison to the pure drug by electrospraying method. Entrapment efficiency ranged from 55 to 66% in solvent emulsification/evaporation method (Kushwaha et al., 2013) but the optimum electrosprayed nanoparticles obtained in the present study showed 97.1 ± 17.1% of entrapment efficiency (Table 3). Co-ground mixture method significantly increased plasma exposures of RH than milled method in animals (Jagadish et al., 2010). Also, Bikiaris et al. (2009) reported novel biodegradable polyesters improved efficacy of the RH nanoparticles. Dissolution rate and extent of the RH was increased with *co*-ground mixtures of drug and poly vinyl pyrrolidones (Garg et al., 2009).

With this increment in RH, it is expected that the enhanced solubility may cause significant increase in the bioavailability of this drug. The results of Table 4 show a 7.5-fold enhancement in $AUC_{0-\infty}$ of the drug using electrosprayed RH. In Kushwaha et al. (2013) study, despite 60% of the orally administered RH was absorbed but its absolute plasma bioavailability was < 3% because of its poor aqueous solubility. The extent of the mean plasma exposures of RH was 5-fold higher in animals treated with RH loaded SLN compared to animals treated with RH pure drug. The mean plasma AUC_{0-24} in animals treated with RH loaded SLN and pure RH was 2063.26 ± 94.4 ng·h/ml and 409.6 ± 34.51 ng·h/ml, respectively. The peak plasma concentration (C_{max}) value for suspension and SLN formulation were 386.33 ± 80.61 ng/ml and 40.67 ± 6.67 ng/ml, respectively (Kushwaha et al., 2013). In another study, self-emulsifying drug delivery system (SEDDS) of RH was developed and oral bioavailability of this drug was determined in rats. SEDDS demonstrated a 4-fold and 2.5-fold higher $AUC_{0-\infty}$ than RH suspension (control) and marketed product, respectively (Thakur et al., 2017). Also by solvent diffusion method nanostructured lipid carriers of RH were produced with 3.75-fold enhancements in in vivo pharmacokinetic parameters (Shah et al., 2016).

Fung et al. (2016) produced electrosprayed CoQ10 microparticles enhancing the dissolution properties, solubility and oral bioavailability of the drug. In another study, Mustapha et al. (2016) generated piroxicam-loaded nanospheres by electrospraying technique using polyvinylpyrrolidone. The optimum formulation was in the ratio of 2:8 of piroxicam: polyvinylpyrrolidone. Their formulation provided about 600-time greater solubility, 15-fold higher release rate and 3-fold higher AUC than the pure piroxicam.

Serum calcium, phosphorous and alkaline phosphatase levels were also significantly decreased in ovariectomized rats orally administered RH nanoparticles (Fig. 9a, b, c). The oral administration of RH loaded in poly(methyl vinyl ether-*co*-maleic acid) nanoparticles to female Wistar rats increased serum biochemical parameters (Fig. 10). As this figure indicates after ovariectomy the serum levels of calcium (Fig. 9a) and phosphorus (Fig. 9b) increased in the untreated group. However, in ovariectomized rats treated with regular RH, this increment was significantly less than that of the untreated group. In rats treated with the RH loaded nanoparticles not only these two elements were not increased but they reduced significantly compared to the other previous groups ($P < 0.05$). Reduction in calcium and phosphorus concentrations in positive control group (treated with estradiol valerate) were more than group treated by regular RH ($P < 0.05$).

5. Conclusion

Electrospraying technique using PMVEMA showed to be a successful method for preparing of RH nanoparticles with considerable solubility. The optimized situation for electrospraying the RH nanoparticles obtained at the voltage of 18.24 kV, the concentration of polymer at 13%, the distance of needle to the collector of 19.69 cm and the flow rate of 0.43 ml/h that produced nanoparticles with the particle size of 201.739 ± 62.60 nm. It increased aqueous solubility of RH from 19.88 ± 0.12 μg/ml to 219.91 ± 14.68 μg/ml and dissolution rate from 11% to ~95% in 10 min. The electrosprayed nanoparticles exhibited smooth morphology with uniform size distribution. Also, electrospraying method improved oral bioavailability of poorly water soluble RH in ovariectomized rats about 7.5-fold. The pharmacodynamic effects of RH in decreasing the calcium, phosphorous and alkaline phosphatase serum levels were also significantly changed compared to the pure drug and reached almost to the effect of positive control group of estradiol valerate. However, further researches are needed to determine the accuracy of the obtained results for human clinical trials. Besides, the results of this study showed the designed nanoparticles in oral route of administration had better bioavailability. In conclusion, the implicated process could be considered as an appropriate method to enhance the solubility, dissolution rate, oral bioavailability and anti-osteoporotic effects of oral RH.

Acknowledgements

The authors appreciate financial support of the project by Vice Chancellery of Research of Isfahan University of Medical Sciences (394690).

Conflict of interest

The authors declare no conflict of interest.

References

Alehosseini, A., Ghorani, B., Sarabi-Jamab, M., Tucker, N., 2017. Principles of electrospraying: a new approach in protection of bioactive compounds in foods. Crit. Rev. Food Sci. Nutr. 1–18.
Anitha, A., Maya, S., Deepa, N., Chennazhi, K., Nair, S., Tamura, H., Jayakumar, R., 2011. Efficient water soluble O-carboxymethyl chitosan nanocarrier for the delivery of curcumin to cancer cells. Carbohydr. Polym. 83, 452–461.
Arya, N., Chakraborty, S., Dube, N., Katti, D.S., 2009. Electrospraying: a facile technique for synthesis of chitosan-based micro/nanospheres for drug delivery applications. J Biomed Mater Res B Appl Biomater 88, 17–31.
Bikiaris, D., Karavelidis, V., Karavas, E., 2009. Novel biodegradable polyesters. Synthesis and application as drug carriers for the preparation of raloxifene HCl loaded nanoparticles. Molecules 14, 2410–2430.
Bock, N., Woodruff, M.A., Hutmacher, D.W., Dargaville, T.R., 2011. Electrospraying, a reproducible method for production of polymeric microspheres for biomedical applications. Polymers 3, 131–149.
Elsheikh, M.A., Elnaggar, Y.S., Gohar, E.Y., Abdallah, O.Y., 2012. Nanoemulsion liquid preconcentrates for raloxifene hydrochloride: optimization and in vivo appraisal. Int. J. Nanomedicine 7, 3787–3802.
Fung, W.Y., Liong, M.T., Yuen, K.H., 2016. Preparation, in-vitro and in-vivo characterisation of CoQ10 microparticles: electrospraying-enhanced bioavailability. J. Pharm. Pharmacol. 68, 159–169.
Garg, A., Singh, S., Rao, V., Bindu, K., Balasubramaniam, J., 2009. Solid state interaction of raloxifene HCl with different hydrophilic carriers during co-grinding and its effect on dissolution rate. Drug Dev. Ind. Pharm. 35, 455–470.
Hao, X., Lu, X., Li, Z., Zhao, Y., Shang, T., Yang, Q., Wang, C., Li, L., 2006. Effects of the electrospray ionization parameters on the formation and morphology of colloidal microspheres of polyacrylonitrile. J. Appl. Polym. Sci. 102, 2889–2893.
Hao, S., Wang, Y., Wang, B., 2014. Sinking-magnetic microparticles prepared by the electrospray method for enhanced gastric antimicrobial delivery. Mol. Pharm. 11, 1640–1650.
Hartman, R., Brunner, D., Camelot, D., Marijnissen, J., Scarlett, B., 2000. Jet break-up in electrohydrodynamic atomization in the cone-jet mode. J. Aerosol Sci. 31, 65–95.
Higuchi, T., Connoras, K.A., 1965. Phase-solubility techniques. Adv. Anal. Chem. Instrum. 4, 117–210.
Hu, C., Liu, S., Li, B., Yang, H., Fan, C., Cui, W., 2013. Micro-/nanometer rough structure of a superhydrophobic biodegradable coating by electrospraying for initial anti-bioadhesion. Adv. Healthc. Mater. 2, 1314–1321.
Jagadish, B., Yelchuri, R., Tangi, H., Maroju, S., RAO, V.U., 2010. Enhanced dissolution and bioavailability of raloxifene hydrochloride by co-grinding with different super-disintegrants. Chem. Pharm. Bull. 58, 293–300.
Jahangiri, A., Davaran, S., Fayyazi, B., Tanhaei, A., Payab, S., Adibkia, K., 2014. Application of electrospraying as a one-step method for the fabrication of triamcinolone acetonide-PLGA nanofibers and nanobeads. Colloids Surf. B: Biointerfaces 123, 219–224.
Jaworek, A., 2007. Micro-and nanoparticle production by electrospraying. Powder Technol. 176, 18–35.
Jia, Z., Lin, P., Xiang, Y., Wang, X., Wang, J., Zhang, X., Zhang, Q., 2011. A novel nanomatrix system consisted of colloidal silica and pH-sensitive polymethylacrylate

improves the oral bioavailability of fenofibrate. Eur. J. Pharm. Biopharm. 79, 126–134.
Kakran, M., Sahoo, N., Li, L., 2011. Dissolution enhancement of quercetin through nanofabrication, complexation, and solid dispersion. Colloids Surf. B: Biointerfaces 88, 121–130.
Kerdsakundee, N., Li, W., Martins, J.P., Liu, Z., Zhang, F., Kemell, M., Correia, A., Ding, Y., Airavaara, M., Hirvonen, J., Wiwattanapatapee, R., Santos, H.A., 2017. Multifunctional nanotube-mucoadhesive poly(methyl vinyl ether-co-maleic acid)@hydroxypropyl methylcellulose acetate succinate composite for site-specific oral drug delivery. Adv. Healthc. Mater. 6 (20), 1–12.
Kushwaha, A.K., Vuddanda, P.R., Karunanidhi, P., Singh, S.K., Singh, S., 2013. Development and evaluation of solid lipid nanoparticles of raloxifene hydrochloride for enhanced bioavailability. Biomed. Res. Int. 2013, 584549.
Luo, C.F., Yuan, M., Chen, M.S., et al., 2011. Pharmacokinetics, tissue distribution and relative bioavailability of puerarin solid lipid nano-particles following oral administration. Int. J. Pharm. 410 (1–2), 138–144.
Moghadam, H., Samimi, M., Samimi, A., Khorram, M., 2009. Study of parameters affecting size distribution of beads produced from electro-spray of high viscous liquids. Iran J. Chem. Eng. 6, 88–98.
Mustapha, O., Din, F.U., Kim, D.W., Park, J.H., Woo, K.B., Lim, S.J., Youn, Y.S., Cho, K.H., Rashid, R., Yousaf, A.M., Kim, J.O., Yong, C.S., CHOI, H.G., 2016. Novel piroxicam-loaded nanospheres generated by the electrospraying technique. Physicochemical characterisation and oral bioavailability evaluation. J. Microencapsul. 33, 323–330.
Narayan, R., Pednekar, A., Bhuyan, D., Gowda, C., Koteshwara, K.B., Nayak, U.Y., 2017. A top-down technique to improve the solubility and bioavailability of aceclofenac in vitro and in vivo studies. Int. J. Nanomedicine 12, 4921–4935.
Newa, M., Bhandari, K.H., Li, D.X., Kim, J.O., Yoo, D.S., Kim, J.A., Yoo, B.K., Woo, J.S., Lyoo, W.S., Yong, C.S., Choi, H.G., 2008. Preparation and evaluation of immediate release ibuprofen solid dispersions using polyethylene glycol 4000. Biol. Pharm. Bull. 31, 939–945.
Nguyen, D.N., Clasen, C., Van Den Mooter, G., 2016. Pharmaceutical applications of electrospraying. J. Pharm. Sci. 105, 2601–2620.
Pathak, S., Gupta, B., Poudel, B.K., Tran, T.H., Regmi, S., Pham, T.T., Thapa, R.K., Kim, M.S., Yong, C.S., Kim, J.O., Jeong, J.H., 2016. Preparation of high-payload, prolonged-release biodegradable poly(lactic-*co*-glycolic acid)-based tacrolimus microspheres using the single-jet electrospray method. Chem. Pharm. Bull.(Tokyo) 64, 171–178.
Patil, P.H., Belgamwar, V.S., Patil, P.R., Surana, S.J., 2013. Solubility enhancement of raloxifene using inclusion complexes and cogrinding method. J. Pharm. 2013, 527380.
Reis, C.P., Neufeld, R.J., Ribeiro, A.J., Veiga, F., 2006. Nanoencapsulation I. Methods for preparation of drug-loaded polymeric nanoparticles. Nanomedicine 2 (1), 8–21.
Roush, K., 2011. Prevention and treatment of osteoporosis in postmenopausal women: a review. Am. J. Nurs. 111 (8), 26–35.
Shah, N., Seth, A.K., Balaraman, R., 2015. Bioavailability enhancement of poorly soluble raloxifene by designing inclusion complex with β–cyclodextrin. Int. J. Pharm. Pharm. Sci. 7 (8), 205–211 (Jun 20).
Shah, N.V., Seth, A.K., Balaraman, R., Aundhia, C.J., Maheshwari, R.A., Parmar, G.R., 2016. Nanostructured lipid carriers for oral bioavailability enhancement of raloxifene. Design and in vivo study. J. Adv. Res. 7, 423–434.
Shahbazi, M.A., Almeida, P.V., Mäkilä, E., Correia, A., Ferreira, M.P.A., Kaasalainen, M., Salonen, J., Hirvonen, J., Santos, H.A., 2014. Poly(methyl vinyl ether-*alt*-maleic acid)-functionalized porous silicon nanoparticles for enhanced stability and cellular internalization. Macromol. Rapid Commun. 35 (6), 624–629.
Silva, B.C., Bilezikian, J.P., 2011. New approaches to the treatment of osteoporosis. Annu. Rev. Med. 62, 307–322.
Smeets, A., Clasen, C., Mooter, G.V.D., 2017. Electrospraying of polymer solutions. Study of formulation and process parameters. Eur. J. Pharm. Biopharm. 119, 114–124.
Sosnik, A., 2014. Production of drug-loaded polymeric nanoparticles by electrospraying technology. J. Biomed. Nanotechnol. 10, 2200–2217.
Sultan, N., Rao, J., 2011. Association between periodontal disease and bone mineral density in postmenopausal women: a cross sectional study. Med. Oral Patol. Oral Cir. Bucal. 16 (3), e440–e447.
Suthar, A.K., Solanki, S.S., Dhanwani, R.K., 2011. Enhancement of dissolution of poorly water soluble raloxifene hydrochloride by preparing nanoparticles. J. Adv. Pharm. Educ. Res. 2, 189–194.
Thakkar, H., Nangesh, J., Parmar, M., Patel, D., 2011. Formulation and characterization of lipid-based drug delivery system of raloxifene-microemulsion and self-microemulsifying drug delivery system. J. Pharm. Bioallied Sci. 3, 442–448.
Thakur, P.S., Singh, N., Sangamwar, A.T., Bansal, A.K., 2017. Investigation of need of natural bioenhancer for a metabolism susceptible drug-raloxifene, in a designed self-emulsifying drug delivery system. AAPS PharmSciTech. http://dx.doi.org/10.1208/s12249-017-0732-2.
Tran, T.H., Poudel, B.K., Marasini, N., Chi, S.C., Choi, H.G., Yong, C.S., Kim, J.O., 2013. Preparation and evaluation of raloxifene-loaded solid dispersion nanoparticle by spray-drying technique without an organic solvent. Int. J. Pharm. 443 (1-2), 50–57 (Feb 25).
Trotta, M., Cavalli, R., Trotta, C., Bussano, R., Costa, L., 2010. Electrospray technique for solid lipid-based particle production. Drug Dev. Ind. Pharm. 36, 431–438.
Uebelhart, B., Herrmann, F., Rizzoli, R., 2009. Effects of the SERM raloxifene on calcium and phosphate metabolism in healthy middle-aged men. Clin. Cases Miner. Bone Metab. 6, 163–168.
Wempe, M.F., Wacher, V.J., Ruble, K.M., Ramsey, M.G., Edgar, K.J., Buchanan, N.L., Buchanan, C.M., 2008. Pharmacokinetics of raloxifene in male Wistar–Hannover rats. Influence of complexation with hydroxybutenyl-beta-cyclodextrin. Int. J. Pharm. 346, 25–37.
Wu, Y., Duong, A., Lee, L.J., Wyslouzil, B.E., 2012. Electrospray production of nanoparticles for drug/nucleic acid delivery. In: The Delivery of Nanoparticles, http://dx.doi.org/10.5772/36672.
Yousaf, A.M., Mustapha, O., Kim, D.W., Kim, D.S., Kim, K.S., Jin, S.G., Yong, C.S., Youn, Y.S., Oh, Y.-K., Kim, J.O., Choi, H.-G., 2016. Novel electrosprayed nanospherules for enhanced aqueous solubility and oral bioavailability of poorly water-soluble fenofibrate. Int. J. Nanomedicine 11, 213–221.
Zamani, M., Prabhakaran, M.P., Varshosaz, J., Mhaisalkar, P.S., Ramakrishna, S., 2016. Electrosprayed montelukast/poly(lactic-*co*-glycolic acid) particle based coating. A new therapeutic approach towards the prevention of in-stent restenosis. Acta Biomater. 42, 316–328.
Zhou, F.-L., Hubbard Cristinacce, P.L., Eichhorn, S.J., Parker, G.J., 2016. Preparation and characterization of polycaprolactone microspheres by electrospraying. Aerosol Sci. Technol. 50, 1201–1215.